Progress on laser plasma accelerator development using transversely and longitudinally shaped plasmas

Wim P. Leemans [a,b,*], E. Esarey [a,b], C.G.R. Geddes [a], Cs. Toth [a], C.B. Schroeder [a], K. Nakamura [a,b], A.J. Gonsalves [a], D. Panasenko [a], E. Cormier-Michel [a], G.R. Plateau [a,c], C. Lin [a,d], D.L. Bruhwiler [e], J.R. Cary [e,f]

[a] *Lawrence Berkeley National Laboratory, Berkeley, CA 94720, USA*
[b] *University of Nevada, Reno, NV 89557, USA*
[c] *École polytechnique, 91128 Palaiseau cedex, France*
[d] *Peking University, Beijing 100871, China*
[e] *Tech-X Corporation, Boulder, CO 80303, USA*
[f] *University of Colorado, Boulder, CO 80309, USA*

Abstract

A summary of progress at Lawrence Berkeley National Laboratory is given on: (1) experiments on down-ramp injection; (2) experiments on acceleration in capillary discharge plasma channels; and (3) simulations of a staged laser wakefield accelerator (LWFA). Control of trapping in a LWFA using plasma density down-ramps produced electron bunches with absolute longitudinal and transverse momentum spreads more than ten times lower than in previous experiments (0.17 and 0.02 MeV/c FWHM, respectively) and with central momenta of 0.76 ± 0.02 MeV/c, stable over a week of operation. Experiments were also carried out using a 40 TW laser interacting with a hydrogen-filled capillary discharge waveguide. For a 15 mm long, 200 μm diameter capillary, quasi-monoenergetic bunches up to 300 MeV were observed. By detuning discharge delay from optimum guiding performance, self-trapping was found to be stabilized. For a 33 mm long, 300 μm capillary, a parameter regime with high energy bunches, up to 1 GeV, was found. In this regime, peak electron energy was correlated with the amount of trapped charge. Simulations show that bunches produced on a down-ramp and injected into a channel-guided LWFA can produce stable beams with 0.2 MeV/c-class momentum spread at high energies.

Résumé

Progrès dans le développement d'accélérateurs laser-plasma utilisant des plasmas profilés transversalement et longitudinalement. On présente un résumé des progrès obtenus au Lawrence Berkeley National Laboratory sur : (1) les expériences sur l'injection dans une rampe de densité décroissante ; (2) les expériences sur l'accélération dans des canaux de plasmas de décharges capillaires ; et (3) les simulations d'accélérateur par champ de sillage laser (LWFA) en configuration multi-étages. Le contrôle du piégeage dans un LWFA à l'aide de rampes de densité décroissante produit des paquets d'électrons avec des dispersions de moment cinétique longitudinal et transversal plus de dix fois plus faibles que dans des expériences antérieures (respectivement 0,17 and 0,02 MeV/c FWHM) avec une valeur centrale de $0,76 \pm 0,02$ MeV/c, stable sur la durée de la semaine d'expérience. Des expériences ont également été faites à l'aide d'un laser de 40 TW interagissant avec un guide d'onde constitué par une décharge

* Corresponding author.
E-mail address: WPLeemans@lbl.gov (W.P. Leemans).

capillaire d'hydrogène. Pour un capillaire de longueur 15 mm et de diamètre 200 µm, des électrons quasi-monoénergétiques atteignant 300 MeV ont été observés. En jouant sur le délai du temps d'allumage de la décharge et en s'écartant ainsi des performances optimales de guidage, l'auto piégeage a pu être stabilisé. Pour un capillaire de longueur 33 mm et de diamètre 300 µm, un régime de paramètres avec des électrons atteignant 1 GeV a été trouvé. Dans ce régime, l'énergie maximum des électrons a été corrélée avec la quantité d'électrons piégés. Les simulations ont montré que des paquets d'électrons produits dans une rampe de densité décroissante et injectés dans un guide dans un LWFA peuvent constituer des faisceaux stables de haute énergie avec des dispersions en moment de l'ordre de 0,2 MeV/c.

Keywords: Laser-driven electron acceleration

Mots-clés : Accélération laser d'électrons

1. Introduction

Laser wakefield accelerators (LWFAs) have demonstrated high field gradients, up to hundreds of GV/m, reducing accelerating distances by a thousandfold compared to conventional technologies [1]. The laser ponderomotive (radiation) pressure drives a plasma density wave (wake), whose longitudinal field can "self-trap" and accelerate electrons from the plasma. Self-trapped LWFA experiments produced bunches with few MeV/c momentum spreads near 100 MeV/c by extending the laser propagation distance using a guiding channel [2] or large spot size [3,4]. Channel guided LWFAs subsequently produced bunches with ~20 MeV/c longitudinal and 2 MeV/c transverse momentum spread at 1 GeV and stable bunches at 500 MeV [5,6].

In self-trapped experiments, injection, acceleration, and guiding are interdependent, which limits tunability and control of the electron bunch quality. Bunch quality was best when operating at the trapping threshold [3,4,6,7], and relatively stable operation [5,6,8] was only observed in a narrow parameter window. The plasmas used had approximately constant density along the laser propagation direction, so that the wake phase velocity v_ϕ was $\sim v_g$ (the laser group velocity [1]). Using lower plasma density increases v_g and hence v_ϕ, allowing electrons to accelerate to higher energies while remaining in phase with the wake [3–5]. However, for given laser parameters, no self-trapping is observed below a minimum density [3–5], indicating the need for externally controlled injection.

Independent control of electron injection into the wake and of the accelerating structure could increase bunch energy by allowing operation of the accelerator at lower density, while also improving stability and quality by allowing independent tuning of injection. This is important for many applications, which desire momentum spreads below those of present experiments (1–20 MeV/c or few % longitudinal spread and ~0.2–2 MeV/c transverse spread). The short plasma wave wavelength $\lambda_p = \sqrt{\pi c^2 m / e^2 n_e}$, typically ~10–100 µm, determines the size requirement for the injected bunch, where n_e is the plasma density.

Two possible laser-based methods for electron injection are colliding pulse injection [9–11] and down-ramp injection [12]. In colliding pulse injection, additional laser pulses are used to boost the momentum of a group of plasma electrons, allowing them to become trapped in the wake. In down-ramp injection, a decreasing plasma density in the direction of laser propagation is used to slow the plasma wave phase velocity such that localized trapping occurs. Experiments [13] have demonstrated controlled injection using the colliding pulse method and showed tuning of the electron energy by changing the injection location within the plasma. Down-ramp injection experiments have also demonstrated the production of electron bunches with small absolute energy spread [14].

Future LWFA experiments are likely to use a staged approach [15]. In the first stage – the injection stage – a relatively low energy, high quality electron bunch is generated using a laser injection method. In the second (and subsequent) stages, this high quality bunch is accelerated to high energies in a "dark current free" (no additional trapping) manner, while preserving the low emittance and low absolute energy spread of the injected bunch.

In this article we report on progress at the Lawrence Berkeley National Laboratory (LBNL) on (1) experimental studies of down-ramp injection, (2) experimental studies of self-trapping and acceleration in capillary discharge plasma channels, and (3) numerical studies using particle-in-cell simulations of a staged LWFA.

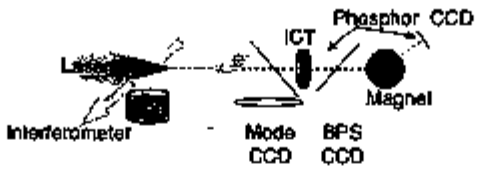

Fig. 1. Setup for density gradient controlled injection. The laser was focused at the downstream edge of a thin slit gasjet where the density is decreasing. An interferometer measured the plasma profile. Electron diagnostics include a magnetic spectrometer, bunch phosphor screen and ICT.

2. Experiments on down-ramp injection

Plasma density gradients with density decreasing in the laser propagation direction (down ramps) have been proposed to control trapping. In such gradients λ_p increases with propagation, causing the wake fronts behind the laser to fall further behind as the laser propagates which decreases the wake phase front velocity v_ϕ [12,16–18]. Use of the gradient separates density (which controls resonance of the plasma wave with laser pulse length [1]) from wake phase velocity, and controls wake phase velocity as a function of propagation distance. The reduced v_ϕ reduces the threshold for trapping by reducing the velocity electrons must achieve to be trapped, and hence allows trapping at lower densities than in uniform plasmas. Such tuning of the trapping threshold has been shown to produce stable electron bunches with an order of magnitude lower absolute momentum spread than other LWFA experiments [14]. The reduced phase velocity also reduces the maximum energy gain however because dephasing occurs quickly. Hence for stable high energy bunches a down ramp region to control trapping should be followed by a long uniform-density plasma for acceleration to high energy.

The experimental setup is displayed in Fig. 1, showing a pulse from the LOASIS Ti:Sapphire laser [19] focused on the downstream edge of a thin slit gas jet oriented transversely to the laser axis. The laser ionized the hydrogen gas and drove a plasma wake. Peak laser power was 10 TW (0.5 J in 47 fs FWHM), focused to a 7.5 μm FWHM spot. The plasma density profile in the laser propagation direction was measured to be Gaussian for densities above the interferometer measurement threshold of $\sim 2 \times 10^{18}$ cm^{-3}, with a peak density of $2.2 \pm 0.3 \times 10^{19}$ cm^{-3} and a FWHM of 750 μm ±100 μm. Simulations show that the wake is excited strongly within a Rayleigh range $Z_R \sim 200$ μm of the laser focus, a small fraction of the jet length. This allowed effective selection of the density gradient where the wake is excited, and hence control of trapping, using laser focus location [14]. Focusing upstream of the jet center produced an increasing or flat density, and electron spectra in this regime have been published previously, showing exponential energy spectra and fluctuating quasi-monoenergetic peaks from self-modulated acceleration [7]. Focusing downstream produced a decreasing density. Electron bunches were characterized by a magnetic spectrometer. The bunch was bent 55° onto a phosphor screen (LANEX) imaged by a CCD, which imaged a momentum range of ±14% about a central momentum determined by the magnet current. Momentum resolution was ±5%. Beam divergence was observed in the out-of-plane direction. Alternatively, divergence and profile in both planes was observed by an insertable bunch phosphor screen (BPS). Charge was determined by cross-correlating the phosphor signals with an integrating current transformer (ICT). Transmitted laser mode and THz bunch length measurements were presented in [14].

Focusing at the downstream edge of the jet, in the density down ramp, produced electron bunches with an order of magnitude lower absolute momentum spread and jitter than previously observed in LWFAs [14], and multiple datasets on different run days showed that accelerator operation was stable and repeatable over a week of operation. Magnetic spectrometer dataset A (Fig. 2) showed bunches with central momentum stable at 0.76 MeV/c ± 0.02 MeV/c RMS and with momentum spread stable at 0.17 MeV/c FWHM (20%) ± 0.02 MeV/c RMS over 28 sequential and 45 total diagnostic shots. In the undispersed plane, the bunch divergence was 20 mrad FWHM ± 1.8 mrad RMS, and pointing deviation was 1.5 mrad RMS.

Bunch divergence in both planes (momentum integrated) was measured on the insertable BPS phosphor (Fig. 3) [20]. A small-divergence bunch is visible surrounded by a broad background. The small-divergence feature has a divergence of 26 (14) mrad in the horizontal (vertical) plane with RMS deviations of ±1.8 (2.5) mrad over 31 shots. Bunch pointing showed 1.8 (1.2) mrad RMS and 8 (5) mrad peak-to-peak deviations in the horizontal (vertical) plane. Deviations in pointing and divergence are much less than the beam divergence. Vertical data agree with measurements from the magnetic spectrometer, indicating that the narrow feature is the MeV bunch. The broad

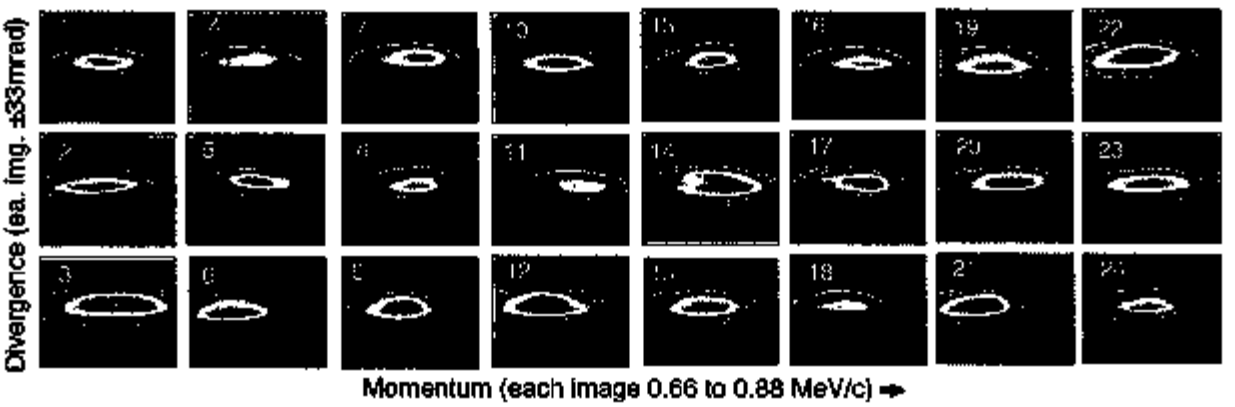

Fig. 2. Sequential magnetic spectra with the laser focus in the density down ramp, from dataset A, display stable bunch performance (showing the 24 shots with the same magnet setting out of the 45 shots in this sequence).

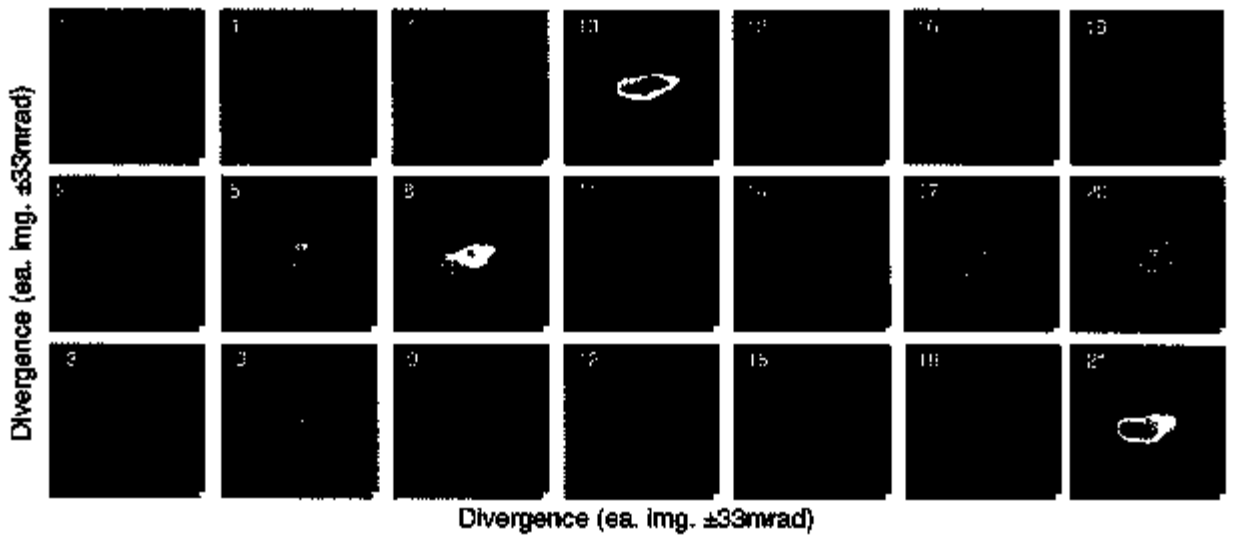

Fig. 3. Sequential electron bunch profiles with the laser focus in the density down ramp, from dataset A. The black solid contour indicates the small-divergence feature (70% of peak). The + indicates the centroid of this feature relative to the mean centroid over all shots (+). Images are plotted on a fixed scale to show charge variation and stability (showing 21 of the 31 shots in this sequence).

background is likely lower momentum electrons. The observed divergence indicates transverse bunch momenta of ~0.02 MeV/c, much lower than the 0.3–2 MeV/c in conventional self-trapped experiments [2,5].

The signals on the magnetic spectrometer and the narrow divergence feature on the BPS phosphor were correlated to ICT charge measurements to extract the charge of the bunch at 0.76 MeV/c. This gave Q_{bunch} of 0.3–1 nC. Charge stability was 40% RMS in this dataset.

The central momentum was stable between 0.76 and 0.78 MeV/c, FWHM energy spread between 0.16 and 0.19 MeV/c, and divergence between 17 to 23 mrad over three runs and over a week of clock time. Fig. 4 shows data from a second sequence of 82 shots (set B), measured 123 hours after Fig. 2, demonstrating this stability. This will be important for LWFA applications and has not been previously observed. Charge stability as good as 15% RMS was observed. Variation in charge stability from run to run is likely due to diurnal variation in laser stability and prepulse.

In the data presented in Figs. 2 and 4, a 10 μm silver coated nitrocellulose pellicle transmitted the electron bunch and diverted the laser to a mode imager CCD [21] to measure the laser profile at the plasma exit [14]. A third set of 60 shots (dataset C) taken immediately subsequent to that shown in Fig. 4 and with the mode imager pellicle

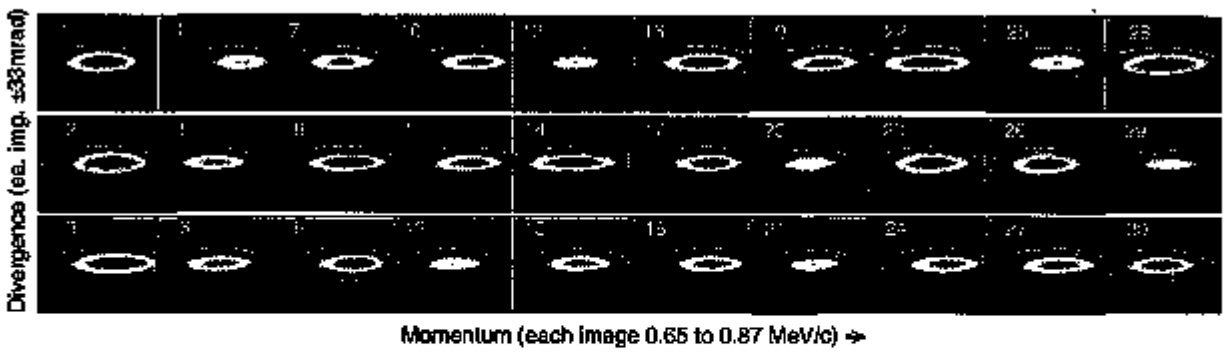

Fig. 4. Sequential magnetic spectra with the laser focus in the density down ramp from run B, 123 hours after run A (showing 30 shots with the same magnet setting out of 82 shots in the sequence).

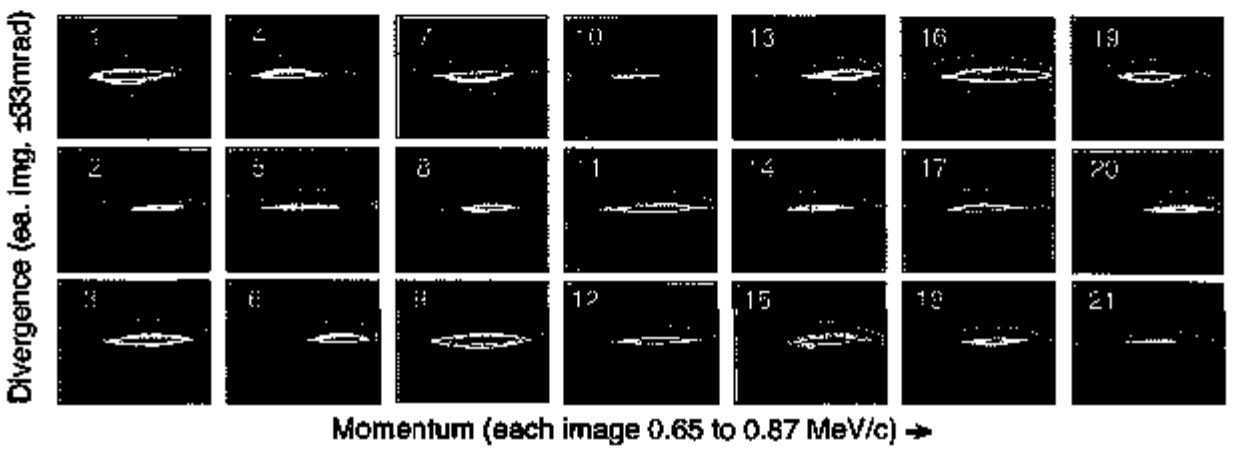

Fig. 5. Sequential magnetic spectra with the laser focus in the density down ramp, and with the mode imager pellicle removed from the beam, from run C, the same day as run B (showing 21 shots with the same magnet setting out of the 60 shots in this sequence).

removed, is displayed in Fig. 5. Visible is a reduction in FWHM divergence by 10–20%, and appearance of a narrow divergence feature (6 mrad) at the 80% contour, indicating that scattering contributed modestly to beam divergence in the measurements, and showing that there is a sub-population of electrons with lower divergence. Longitudinal momentum spread was not affected.

3. Experiments on acceleration with capillary discharge plasma channels

In the first generation of capillary discharge guided LWFA experiments [5,6], accelerator performance was found to exhibit a complicated and sensitive interdependence on input laser and plasma parameters. These parameters included the delay between the onset of the discharge current and arrival of the laser beam (discharge delay t_d), the estimated on-axis plasma density n_0 [22], the peak laser power P, and the capillary diameter. Electron beams with energies of 1 GeV were obtained in a 33 mm long, 300 μm diameter capillary for $P \sim 42$ TW and $n_0 \simeq 4.3 \times 10^{18}$ cm^{-3}. Although 1 GeV beam generation was not stable, a statistical analysis did show a parameter regime where 0.5 GeV e-beams were produced with improved stability by tightly controlling the input parameters for a 33 mm long, 225 μm diameter capillary.

In order to design a next generation apparatus for stable production of higher quality e-beams, with small emittance and high energy and charge, it is critical to untangle this interdependence of input laser and plasma parameters, which requires further parameter exploration and analysis. We next present a performance analysis of the capillary discharge guided LWFA using a 15 mm long, 200 μm diameter and a 33 mm long, 300 μm diameter capillary. Experiments varying capillary length give insight into the trapping and dephasing physics of the capillary discharge guided LWFA.

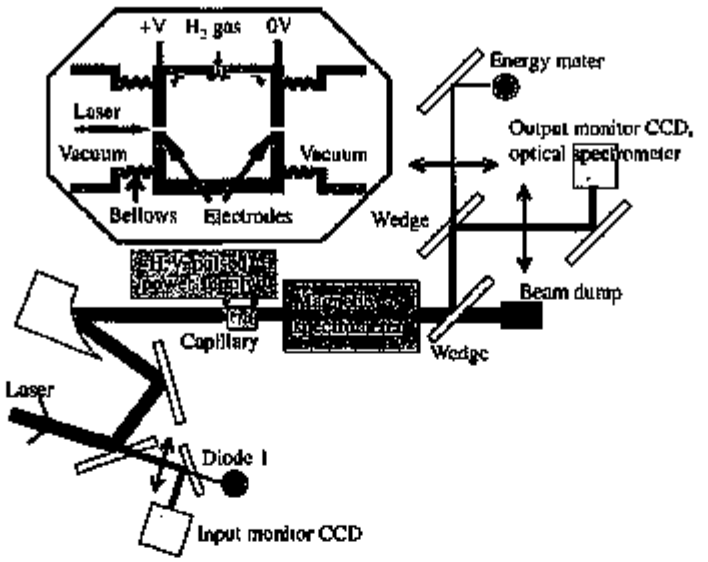

Fig. 6. Schematic diagram of the capillary discharge-guided laser wakefield accelerator and diagnostics. A detail of the capillary discharge unit is in the upper insert, and that of the electron spectrometer can be found in Ref. [23]

The schematic of the capillary discharge guided LWFA experiments is shown in Fig. 6. The laser that was utilized was the short pulse, high peak power and high repetition rate (10 Hz) Ti:Al_2O_3 laser system of the LOASIS facility at LBNL. The laser beam was focused onto the entrance of a capillary discharge waveguide by an f/25 off-axis parabolic mirror. A typical focal spot size (or waist) was $r_0 \simeq 25$ μm containing 60% of the laser energy. Here, a Gaussian transverse profile of $I = I_0 \exp(-2r^2/r_0^2)$ is assumed. Full energy and optimum compression gives $P = 43$ TW ($\tau_{in} \simeq 40$ fs for the FWHM of the intensity pulse), calculated peak intensity $I_0 = 2P/\pi r_0^2 \simeq 2.6 \times 10^{18}$ W/cm^2, and a normalized vector potential $a_0 \simeq 8.6 \times 10^{-10} \lambda[\mu m] I^{1/2}[W/cm^2] \simeq 1.1$.

The capillary waveguide was laser-machined in a sapphire plate. Hydrogen gas was introduced into the capillary using two gas slots as shown in Fig. 6 (insert). A discharge was struck between electrodes located at each end of the waveguide, using a high voltage pulsed power supply with a 4 nF capacitor charged to between 15 and 18 kV. Measurements showed that a fully ionized, approximately parabolic channel was formed on axis [22]. This fully ionized feature was also confirmed by the absence of ionization induced blueshifting of the transmitted laser spectrum when a low power (<0.2 TW) laser pulse was guided.

The electron beams generated were characterized by an electron spectrometer utilizing a round dipole magnet with a maximum magnetic field of 1.25 T and effective radius of 195 mm. The magnetic spectrometer allowed simultaneous measurement of the laser pulse and e-beam due to its large gap, and single shot measurement of electrons from 0.01 GeV to 0.14 GeV (bottom view) and 0.17 GeV to 1.1 GeV (forward view) [23]. The laser energy was monitored both before and after the interaction to evaluate the guiding efficiency and guided beam quality. The laser output spectrum was measured by a broadband optical spectrometer which covers a wavelength range of 320 to 1000 nm in a single shot.

In experiments using a 15 mm long, 200 μm diameter capillary, the guiding performance and e-beam generation showed clear dependence on the discharge delay. Shown in Fig. 7(a) are the discharge delay dependence of several binned optical spectra. The center is defined as the light within the frequency bandwidth of $770 \leqslant \lambda \leqslant 835$ nm, and 100% of incident light was within this band. The red (blue) shift is defined as $835 < \lambda < 1100$ nm ($320 < \lambda < 770$ nm). The input laser parameters were 0.9 J (±3%), 41 fs ($a_0 \sim 0.8$), and the plasma density was 2.5 or 3.7×10^{18} cm^{-3}. For relatively short discharge delay ($t_d < 130$ ns), significant red shift and moderate blue shift were observed, consistent with laser pulse modulation and energy deposition onto the plasma via wakefield generation. For longer discharge delay ($t_d > 130$ ns), the optical spectrum exhibited significant blue shift as well as red-shift, and the transmission efficiency dropped.

The probability of observing any e-beams on the electron spectrometer in the range from 0.01 to 1.1 GeV is shown in Fig. 7(b) by dashed lines. For $n_0 \sim 2.5 \times 10^{18}$ cm^{-3}, no electron beams were observed for $t_d < 110$ ns and trans-

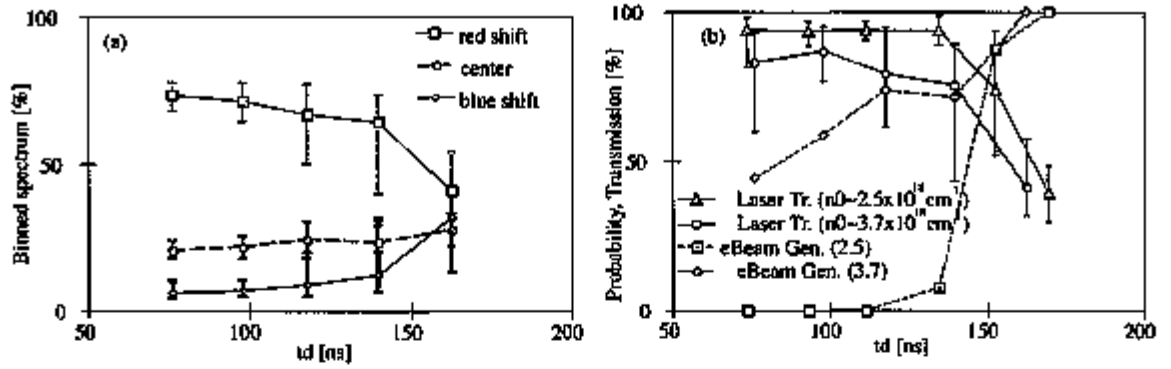

Fig. 7. Results for 15 mm long, 200 μm diameter capillary: (a) Binned transmitted optical spectrum versus discharge delay for $n_0 \sim 2.5 \times 10^{18}$ cm^{-3}. The center is defined as the light within the frequency bandwidth of $770 \leqslant \lambda \leqslant 835$ nm. The red (blue) shift is defined as $835 < \lambda < 1000$ nm ($320 < \lambda < 770$ nm). (b) Transmission efficiency of laser pulses [solid line, triangles (circles) for $n_0 \sim 2.5(3.7) \times 10^{18}$ cm^{-3}], and the probability of e-beam observation on the electron spectrometer [dashed line, squares (diamonds) for $n_0 \sim 2.5(3.7) \times 10^{18}$ cm^{-3}] versus discharge delay. For both figures, the input laser parameters were 0.9 J (±3%), 41 fs ($a_0 \sim 0.8$). A total of 80 shots were taken for each plasma density. Bars show minimum and maximum points.

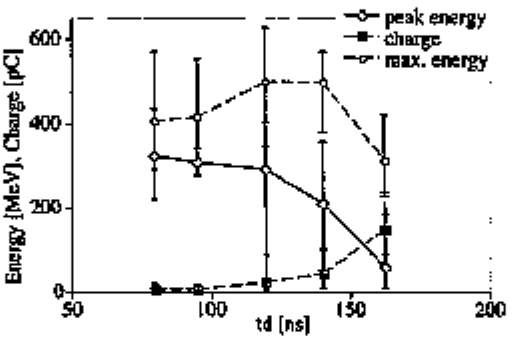

Fig. 8. The peak energy (diamonds), maximum energy (circles), and total charge (squares) versus discharge delay for 15 mm long, 200 μm diameter capillary. Plasma density was $n_0 \sim 3.7 \times 10^{18}$ cm^{-3}, and the laser parameters were 0.9 J (±3%), 41 fs ($a_0 \sim 0.8$). A total of 54 shots were observed with electron beam. Bars show minimum and maximum points.

mission efficiency was high (>80%). This suggests that, although a wakefield was generated based on the observation of significant red-shift, it was not large enough to trap background electrons. Electron beams were observed for longer discharge delay, along with a drop in transmission efficiency and enhanced blue shift. Note that by using higher density plasma ($n_0 \sim 3.7 \times 10^{18}$ cm^{-3}), e-beams were observed for shorter discharge delay without significant blue shift in transmitted optical spectrum.

The peak of the e-beam energy distribution (peak energy), the highest energy in the e-beam energy distribution (maximum energy), and total charge observed on the spectrometer versus discharge delay for $n_0 \sim 3.7 \times 10^{18}$ cm^{-3} are shown in Fig. 8. One can see that relatively high energy (peak energy), low charge e-beams were observed with shorter discharge delay while low energy, high charge beams were observed with longer delay. For longer discharge delay, electron beams occasionally exhibit broadband, multiple peak structure, and significant low energy tail.

Several mechanisms could be responsible for the enhancement of blue shifting, laser transmission loss, and electron trapping observed for longer discharge delay. For longer discharge delay, the amount of ionization, depth of the plasma channel, and plasma density decrease. It has also been suggested that the amount of discharge-ablated material interacting with the laser pulse increased [24]. For a substantial amount of laser pulse energy to be blue shifted by ionization requires the peak intensity of the laser pulse to be within an order of magnitude of the ionization intensity of the ion species with which the pulse interacts. In the case of hydrogen this is 10^{14}–10^{15} W/cm^2, several orders of magnitude lower than the intensity of the laser in the channel. Ablated materials (e.g., aluminum, oxygen) have higher ionization thresholds, and the deteriorated channel may lead to laser ablation of the capillary wall. Alternatively, the blue shifting could be caused by photon acceleration of the back of the laser pulse [25], if it has stretched to a length of

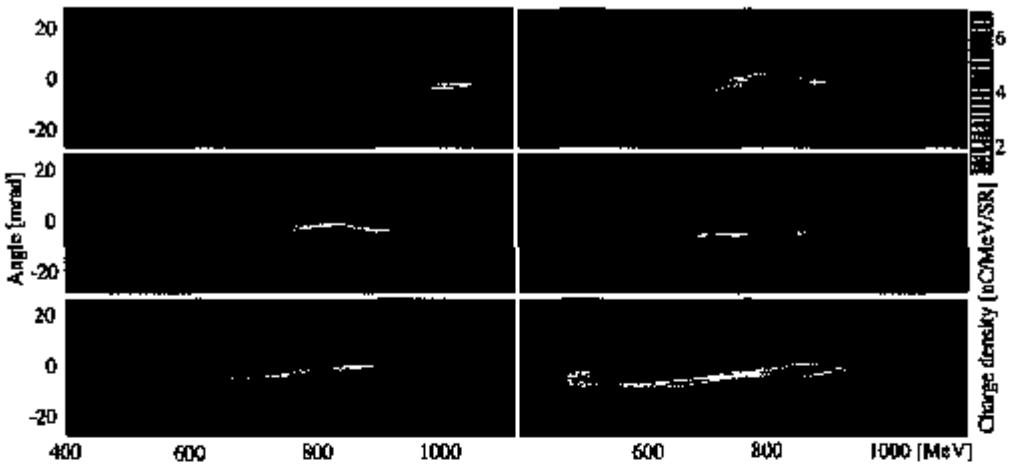

Fig. 9. Representative high energy single shot e-beam spectra for a 33 mm long, 300 μm diameter capillary. The plasma density was $n_0 \sim 5.3 \times 10^{18}$ cm^{-3}, and the laser parameters were 1.5 J (±5.7% RMS), 46 fs ($a_0 \sim 0.8$).

order the plasma wavelength. The reduced laser transmission was likely due to ionization (hydrogen and/or discharge ablated material) and laser leakage from the channel rather than stronger wakefield generation, because of the lower maximum energy observed for longer discharge delay. To explain enhanced trapping, recent studies suggested the interaction with a partially ionized plasma could assist self-trapping [26,27]. Discharge-ablated materials drifting to the axis before the arrival of the laser could contribute to this process. Note that laser-ablated materials could not contribute to this process. Another possible explanation is an increase in the on-axis plasma density due to the deterioration of the channel. Although the amount of ionization decreases for longer discharge delay, the laser pulse was strong enough to ionize hydrogen, so that the on-axis density increases with delay time.

In 2006, generation of e-beams with energies of 1 GeV was reported for a 33 mm long, 300 μm diameter capillary with three gas slots [5,6]. Similar to those results, a parameter regime where e-beams with energies of up to 1 GeV were produced was identified for a 33 mm long, 300 μm diameter capillary with two gas slots. Representative single shot e-beam spectra are shown in Fig. 9. The plasma density was $n_0 \sim 5.3 \times 10^{18}$ cm^{-3}, the laser parameters were 1.5 J (±5.7% RMS), 46 fs ($a_0 \sim 0.93$), and the discharge delay was $t_d \sim 580$ ns. In this parameter regime, 51 shots were taken, and 37 shots produced electrons above 400 MeV. Average peak energy was 713 MeV, and average charge was 6 pC. Since e-beams were often observed with a low energy tail in this regime, only electrons with energy above 400 MeV were taken into account for the analysis. The average laser transmission efficiency was 65%. With this capillary, up to 70% transmission efficiency was observed for 700 ns discharge delay.

The peak energy and maximum energy versus total charge for a 33 mm long, 300 μm diameter capillary are shown in Fig. 10. The peak energy showed clear dependence on the charge, while the maximum energy was somewhat insensitive to charge. One possible explanation of this observation is the beam loading effect. The trapped electron bunch produces a wakefield which modifies the wakefield generated by the laser pulse. For a short, high charge bunch, the head-to-tail variation of the accelerating field can be greater than in the zero charge limit, leading to a larger bunch energy spread. Another possible explanation is that the higher charge beams were trapped over a large phase region in the plasma wave, resulting in a larger head-to-tail wake variation and a larger energy spread. To produce e-beams in a reproducible manner, controlling the amount and the location of electron trapping will be critical.

4. Simulations of staged laser wakefield acceleration

Experiments underway at LBNL are now focusing on a staged LWFA approach in which a down-ramp electron injector is coupled to a capillary discharge plasma channel for acceleration to high energy [15]. Here we report progress on the design and physics of such a staged approached using the results of PIC simulations with the VORPAL [28] framework.

The low phase velocity that stabilizes and controls trapping in down-ramp injection also causes rapid dephasing of the electron bunch, setting the 1 MeV-class maximum energy observed, and requiring injection of these bunches into

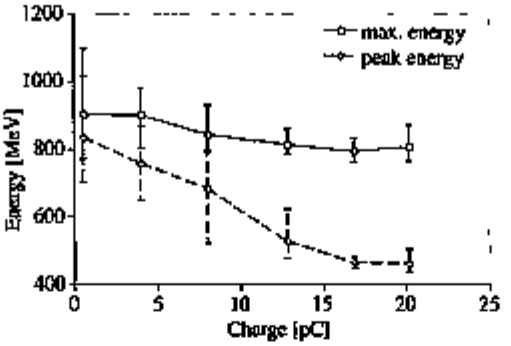

Fig. 10. The peak energy and maximum energy versus charge for 33 mm long, 300 μm diameter capillary. Out of a set of 51 shots, 37 shots were observed with electrons above 400 MeV. Bars show minimum and maximum shots.

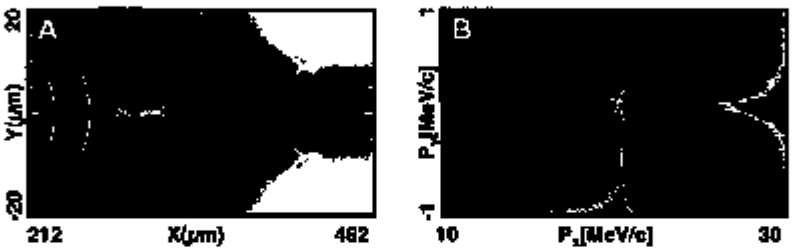

Fig. 11. Simulations merging density gradient injection to an accelerating channel at the location where the electrons dephase in the down ramp. A continuous wake is driven (A) across the transition from the ramp into the channel (plasma wake density, gray) by the laser (red), accelerating particles (yellow). Acceleration in the channel (B) produces 20 MeV bunches while preserving the 0.2 MeV/c momentum spread.

a subsequent LWFA stage to achieve high energy. As λ_p lengthens in the down ramp, the bunch expands to $\geqslant$50 μm in dimension, and this length has been benchmarked to THz radiation measurements [29]. Use of the bunches as an injector therefore requires that the post-accelerating stage be directly coupled to the down ramp at the dephasing point, so that the bunch remains smaller than λ_p in the post-accelerating stage. Use of such a continuous plasma in turn requires that the laser be well transmitted through the down ramp to drive the wake for post acceleration. Experiments [29,14] and simulations (Fig. 11) show that this requirement is met. The transmitted laser mode was similar to the vacuum mode, with no filamentation and with laser transmission of more than 70% when the jet was preionized by an 'ignitor' laser pulse arriving before the drive pulse (ignitor setup shown in [21]).

Simulations ending the down ramp in a plasma channel with uniform axial density immediately after the particles are trapped show that the bunch is accelerated to high energy while preserving its low momentum spread (Fig. 11). Because the bunch is short compared to the plasma wavelength and because beam loading is not severe in this case, the variation of the accelerating field across the bunch is modest and its momentum spread is nearly preserved, producing 0.2 MeV/c class momentum spread at high energy. These simulations have so far shown acceleration to beyond 20 MeV/c (limited by computational time) with 0.18 MeV/c longitudinal and 0.15 MeV/c transverse momentum spread, corresponding to <1% energy spread and <10 mrad divergence. Longer and 3D simulations using the envelope model are in progress to optimize bunch quality. Additional simulations indicate that such post-acceleration nearly preserves absolute momentum spread, which may enable bunches at GeV energies and beyond with <0.1% energy spread.

5. Summary

Research progress at LBNL has been presented on (1) experiments on down-ramp injection, (2) experiments on acceleration in capillary discharge plasma channels, and (3) simulations of staged LWFAs. Experiments demonstrated that plasma gradient control of injection in LWFAs produced bunches with 10- to 100-fold lower momentum spread and variation than previous laser accelerators, and demonstrated day-to-day stability over a week of run time. The bunches displayed central momentum of 0.76 ± 0.02 MeV/c, momentum spread in the longitudinal (transverse)

direction of 0.17 (0.02) MeV/c FWHM, and pointing stability of 2 mrad or 0.002 MeV/c RMS. Charge stability between 15 and 45% RMS was observed. The simulated bunch size of ~10 μm long by 5 μm diameter, together with the experimental and simulated divergences (~20 mrad FWHM), implies a normalized emittance on the order of 0.2–0.4π mm-mrad [14], which would be a ten-fold improvement over previous LWFAs.

Relativistic electron beam generation via a capillary discharge guided LWFA was studied by using 15 mm long, 200 μm diameter and 33 mm long, 300 μm diameter capillaries. Generation of quasi-monoenergetic e-beams up to 300 MeV was observed from the 15 mm long capillary, and up to 1 GeV was observed from the 33 mm long capillary. By using longer discharge delay, self-trapping was stabilized for the 15 mm long, 200 μm diameter capillary. This regime could be used to design a stable self-injected, capillary discharge guided LWFA. While reproducible beams have been observed in tightly controlled parameter regime, a controlled mechanism for injection will be important to enhance LWFA performance.

Simulations benchmarked to the experiments showed that by coupling bunches from a down-ramp injector to subsequent channel-guided stages, the low absolute momentum spread was preserved as the bunch accelerated, resulting in high energy beams with 0.2 MeV/c momentum spread and low emittance. This may allow bunches at GeV energies and beyond with <0.1% energy spread. Together with the observed stability over many run days, these properties will benefit many LWFA applications.

Acknowledgements

This work was supported by the Director, Office of Science, High Energy Physics, U.S. Department of Energy under contracts DE-AC02-05CH11231, DE-FC02-07ER41499, DE-FG02-06ER84484, DE-FG03-95ER40926, DE-FG02-01ER41178, DE-FG02-03ER83857, DOE SciDAC, NERSC, and ATLAS programs, National Science Foundation contracts 0113907 and 0614001, and DARPA. We appreciate the contributions of J. van Tilborg, D. Syversrud, J. Wallig, and N. Ybarrolaza.

References

[1] For a review, see E. Esarey, et al., IEEE Trans. Plasma Sci. 24 (1996) 252–288.
[2] C.G.R. Geddes, et al., Nature 431 (2004) 538–541.
[3] S.P.D. Mangles, et al., Nature 431 (2004) 535–538.
[4] J. Faure, et al., Nature 431 (2004) 541–544.
[5] W.P. Leemans, et al., Nat. Phys. 2 (2006) 696–699.
[6] K. Nakamura, et al., Phys. Plasmas 14 (2007) 056708.
[7] C.G.R. Geddes, et al., Phys. Plasmas 12 (2005) 056709.
[8] C.-T. Hsieh, et al., Phys. Rev. Lett. 96 (2006) 095001.
[9] E. Esarey, et al., Phys. Rev. Lett. 79 (1997) 2682–2685.
[10] G. Fubiani, et al., Phys. Rev. E 70 (2004) 016402.
[11] H. Kotaki, et al., Phys. Plasmas 11 (2004) 3296–3302.
[12] S. Bulanov, et al., Phys. Rev. E 58 (1998) R5257.
[13] J. Faure, et al., Nature 444 (2006) 737–739.
[14] C.G.R. Geddes, et al., Phys. Rev. Lett. 100 (2008) 215004.
[15] A.J.W. Reitsma, et al., Phys. Rev. ST-AB 5 (2002) 051301.
[16] R.G. Hemker, N.M. Hafz, M. Uesaka, Phys. Rev. ST-AB 5 (2002) 041301.
[17] H. Suk, N. Barov, J.B. Rosenzweig, E. Esarey, Phys. Rev. Lett. 86 (2001) 1011.
[18] V. Petrillo, L. Serafini, P. Tomassini, Phys. Rev. ST-AB 11 (2008) 070703/1–7.
[19] LOASIS facility (LBNL): http://loasis.lbl.gov/.
[20] For BPS data, a second laser pulse (2 TW) was present from other experiments. Bunch properties were independent of its pointing. Spectrometer data (no second laser), verified the second laser did not affect the bunch.
[21] C.G.R. Geddes, et al., Phys. Rev. Lett. 95 (2005) 145002.
[22] A.J. Gonsalves, et al., Phys. Rev. Lett. 98 (2007) 025002.
[23] K. Nakamura, et al., Rev. Sci. Instrum. 79 (2008) 053301.
[24] A.J. Gonsalves, Ph.D. thesis, University of Oxford, 2006.
[25] C.D. Murphy, et al., Phys. Plasmas 13 (2006) 033108.
[26] T.P. Rowlands-Rees, et al., Phys. Rev. Lett. 100 (2008) 105005.
[27] E. Oz, et al., Phys. Rev. Lett. 98 (2007) 084801.
[28] C. Nieter, J. Cary, J. Comp. Phys. 196 (2004) 448–473.
[29] G. Plateau, et al., in: Proc. Part. Accel. Conf., IEEE, Piscataway, NJ, 2007.